ACS APPLIED MATERIALS & INTERFACES

Research Article

www.acsami.org

Electrochemically Active Thin Carbon Films with Enhanced Adhesion to Silicon Substrates

Pengfei Niu,[†] Laura Asturias-Arribas,[†] Martí Gich,[*,†] César Fernández-Sánchez,[*,‡] and Anna Roig[†]

[†]Institut de Ciència de Materials de Barcelona, ICMAB (CSIC), Campus UAB, 08193 Bellaterra, Spain

[‡]Instituto de Microelectrónica de Barcelona, IMB-CNM (CSIC), Campus UAB, 08193 Bellaterra, Spain

Supporting Information

ABSTRACT: Thin carbon films deposited on technologically relevant substrates, such as silicon wafers, can be easily implemented in miniaturized electrochemical devices and used for sensing applications. However, a major issue in most carbon films is the weak film/substrate adhesion that shortens the working device lifetime. This paper describes the facile preparation of robust thin carbon films on silicon substrates by one-pot sol−gel synthesis. The improved adherence of these carbon films is based on the incorporation of silica through the controlled synthesis of a resorcinol/formaldehyde gel modified with aminopropyltriethoxysilane. The films demonstrate excellent adhesion to the silicon substrate, good homogeneity, excellent electrical conductivity and superior electrochemical performance. Moreover, this approach opens the door to the fabrication of carbon thin-film electrodes by photolithographic techniques.

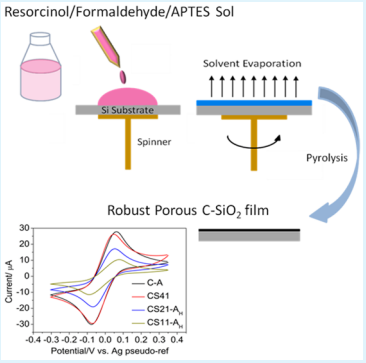

KEYWORDS: *carbon films, silica, sol−gel, adhesion, electrochemical sensors, hybrid materials*

1. INTRODUCTION

Carbon-based materials have attracted much attention as electrodes for electrochemical sensors because of its low cost, wide potential window, relatively inert electrochemistry and electrocatalytic activity in a wide range of redox reactions involving inorganic, organic and biological molecules.[1,2] Most carbon electrodes are prepared by processing bulk carbonaceous materials, such as graphite and glassy carbon,[3] or carbon nanomaterials,[4,5] including nanotubes[6] or graphene.[7] The introduction of these carbon materials into an electrode device varies from sensor to sensor depending on the eventual device application. For instance, to prepare carbon paste electrodes,[8] which are widely used for research purposes, the carbon particles can be easily dispersed in a viscous liquid vehicle. By contrast, the industrial mass production of screen printed electrodes (SPE), such as the ones used in glucose test strips for diabetes,[9] requires engineering complex carbon-based inks by incorporating binders and other additives to the liquid carrier. The widely used SPEs[10] are thick-film electrodes which were developed to meet the needs of disposable miniaturized electrochemical probes to enable on-site analyses.[11] The growing trend toward enabling automated on-site monitoring in real time and for extended periods of time has placed miniaturized robust electrodes in the limelight. SPEs are not tailored to meet these specific needs as the presence of binders and other additives are at the origin of an accelerated deterioration of electrode performance. In this context, miniaturized thin-film carbon electrodes are an attractive alternative offering additional advantages, such as improved electrochemical performance, thanks to its nearly pure carbon composition, and the possibility of fabrication using robust and well setup photolithographic based processes.

Deposition of high quality carbon films is critical for the electrochemical sensor application and should meet three important requirements.[12] First, the deposition procedure should be simple and cost-effective. Second, the films have to be robust enough to be patterned by photolithographic techniques, which involve working with reactive solvents and photoresists of different nature. Third, the resulting sensor must be mechanically and chemically robust to withstand exposure to various electrolyte media and multiple electrochemical processes. To fulfill the above-mentioned characteristics, the thin carbon films must demonstrate an excellent interfacial adhesion to the substrate.

A variety of methods have been reported for the preparation of thin carbon films displaying a wide range of structures and properties between those of graphite and diamond[1,2,12] or even more exotic forms of carbon such as nanotubes[13] or graphene.[14] Most of these films have been prepared on technologically relevant substrates such as silicon either by depositions by electron beam evaporation and pyrolysis[15] and films prepared from liquid precursors such as polymers[16] or photoresists.[17] The pyrolysis approach has the advantages of simplicity and low cost and moreover, the so-called pyrolyzed photoresist films (PPF) can be easily patterned by photolithography before pyrolysis. However, a quite common

Received: June 17, 2016
Accepted: October 18, 2016
Published: October 18, 2016

DOI: 10.1021/acsami.6b07347
ACS Appl. Mater. Interfaces 2016, 8, 31092−31099

Table 1. Sol Compositions, Details of the Gelation Process, and Resulting Film Thickness[a]

samples	R (g)	F (mL)	APTES (mL)	ethanol (mL)	HAc (μL)	reaction time (h)	gelation time (h)	film thickness (nm)	cracks on films
CS11-A_{H-1}	0.4	0.54	0.84	2	785	x	0.15	x	x
CS11-A_H	0.4	0.54	0.84	4	785	1	10	∼400	no
CS21-A_H	0.4	0.54	0.42	2	785	1	24	∼400	no
CS41-A_H	0.4	0.54	0.21	2	785	24	72	∼400	no
CS41-A_L	0.4	0.54	0.21	2	50	1	10	∼400	no
CS41	0.4	0.54	0.21	2		0.15	0.5	∼800	no
C-A	0.4	0.54		2	785	120	168	∼350	no

[a]x: Unprocessable. CS: Carbon silica. R: Resorcinol. F: Formaldehyde. HAc: Acetic acid. Reaction time: Time before spin-coating the sol.

shortcoming of carbon electrode patterns prepared by this approach is a weak film/substrate interaction, manifested by film flaking during long-term operation and this represents the most hampering limitation for sensor applications.

Chemical bonding between the film and the substrate is essential to ensure a robust construct. Thus, considering the well-known fact that silica films on silicon (Si) substrates show strong film/substrate adhesion because of the formation of siloxane chemical bonds (−Si−O−Si−),[18] one route to improve the adherence of carbon film on Si substrates is by the incorporation of silica into the carbon matrix. Interestingly, we reported that pyrolyzed organic gels are appealing materials to fabricate electrodes for electrochemical sensors[19] and moreover sol−gel chemistry offers the possibility of mixing the different precursors from carbon and silica at molecular level resulting in homogeneous composite (carbon/silica) hybrid materials.[20−22] In particular, Song et al. have reported on porous carbon/silica films on Si substrates fabricated by spin coating a sol composed of both silica and phenol/formaldehyde, followed by a pyrolysis step,[21] pointing out that the addition of silica into the carbon matrix significantly improved the adhesion of the film on the substrate. Moreover, conductivity of these carbon/silica films up to 40 wt % silica content remained comparable to that of carbon inks commonly used for the preparation of screen printed electrodes. In their approach the carbonaceous and silica sols were synthesized separately and then mixed together. Such approach is time-consuming, requiring a multiple-step process carried out over several days.

Here, we report on the fabrication of hybrid carbon/silica thin films with enhanced interfacial adhesion to silicon/silicon oxide substrates by a one-step sol−gel route. Resorcinol and formaldehyde are used as the carbon source while aminopropyltriethoxysilane (APTES) was selected as the silica source. A homogeneously mixed solution of these three components formed a gel that is spin-coated onto the substrate and converted into a carbon/silica film by controlled pyrolysis. The synthetic conditions to prepare uniform films on silicon/silicon oxide substrates are then optimized. Surface morphology, electrical conductivity, and electrochemical performance of these films are systematically investigated. The films display remarkable enhanced interfacial adhesion to silicon wafers and superior electrochemical properties.

2. EXPERIMENTAL SECTION

2.1. Reagents and Materials. The following chemicals were purchased from Sigma-Aldrich and used as received: resorcinol (m-$C_6H_4(OH)_2$, 99% pure), formaldehyde−water solution (CH_2O, 37 wt %, methanol stabilized), (3-aminopropyl)trimethoxysilane (APTES ≥ 98%), ethanol (96% pure), acetic acid (CH_3COOH, 99.7% pure), potassium ferricyanide, and potassium ferrocyanide 99% pure and potassium nitrate (purity >99.0%), also from Sigma-Aldrich were employed for the electrochemical characterization.

Five hundred micrometer-thick 4-in. silicon wafers were thermally oxidized at 1000 °C to get a 1 μm thick silica layer, labeled as silicon/silicon oxide wafer. The oxide-terminated silicon wafer was diced into 2 × 2 cm^2 substrates. Prior to use, the substrate was thoroughly cleaned in hot piranha solution and rinsed in distilled water.

2.2. Preparation of Carbon/Silica Films. The preparation of carbon/silica films involves three steps, namely, (1) sol preparation, (2) spin-coating an organic/silica film, and (3) carbonization. The nature of the sol is critical for the successful deposition of the films by spin-coating. The influence of the sol in the final thickness of the film is presented in detail in section 2.3. Table 1 lists the composition of the sols employed for producing the carbon films. In step 1, APTES was first dissolved in ethanol or an ethanol/acetic acid mixture in a glass container, and then resorcinol and formaldehyde were added successively. The mixture was stirred continuously at room temperature until a clear homogeneous solution was formed. The resorcinol/APTES molar ratio was varied between 1 and 4. The relative molar content of resorcinol and APTES are indicated in the sample labeling by the two digits following carbon silica, respectively. The labeling of the films shown in Table 1 also takes into account if relatively high (A_H) (785 μL) or low quantities (A_L) (50 μL) of acetic acid were used in the preparation of the sol, adding A_H and A_L, respectively, in the label. For comparison, a carbon film, labeled C−A, was also prepared using a sol containing only carbon precursor.

In step 2, the sols were spin-coated onto 2 × 2 cm^2 silica/silicon oxide. Then, gels were deposited by spin coating using rotation speeds from 1000 to 4000 rpm. We observed that the average film thickness before pyrolysis decreased when increasing the rotation speed, tending to level off above 3000 rpm. To obtain reproducible resorcinol/formaldehyde/SiO_2 films, the spin-coating with the sols was always performed at 4000 rpm for 45 s.

The viscosity of the sols, which is closely related with its composition, dramatically increases with reaction time and plays a decisive role in the quality of the coated film and its final thickness. To obtain continuous and crack-free films, the viscosity of the sols at different reaction times was measured with a HAAKE RheoStress RS600 rheometer in velocity control mode with a shear rate of 2880 s^{-1} during 30 s at 20 °C. Sols with viscosities ranging from 6 to 10 mPa·s resulted in good quality crack-free films with thicknesses between 400 and 800 nm. However, spinning sols with viscosities higher than 11 mPa·s produced after pyrolysis cracked films thicker than 1000 nm (see Figure S1). The viscosities were adjusted to suitable values by controlling reaction times at room temperature before spinning. The suitable reaction times that were used to obtain crack-free C/SiO_2 films of around 400 nm thick are included in Table 1 for all the sol compositions.

In step 3, immediately after spin-coating, the gels were placed in an oven at 60 °C for more than 4 h for gel aging. Afterward, they were placed in a quartz tube and pyrolyzed under Ar + H_2 (95% + 5%) atmosphere to convert them into C/SiO_2 films. For carbonization, the furnace temperature was raised to 1000 °C at a rate of 200 °C/h, maintaining it at this temperature for 2 h and then switching the power off to let the furnace cool down to room temperature. During the pyrolysis process, the gas flow rate was 100 cm^3/min.

DOI: 10.1021/acsami.6b07347
ACS Appl. Mater. Interfaces 2016, 8, 31092−31099

2.3. Film Characterization. The chemical compositions and the nature of the C and Si bonds of the surface of C/SiO_2 films were analyzed by X-ray photoelectron spectroscopy (XPS) employing AlKa radiation. Scanning electron microscopy (SEM) was used to study the chemical homogeneity of the films. The surface morphology of the C/SiO_2 films was observed by optical microscopy and atomic force microscopy (AFM) using an Agilent 5100 equipment and a KLA profilometer. The thickness of the spin-coated films before and after carbonization was measured with the profilometer on a zone of the film that had been intentionally scratched with a razor blade (see Figure S2 for a representative 3D profilometric image of a measured film after pyrolysis). The microstructure of the films was studied by SEM at 10 kV (Carl Zeiss Auriga-40 and FEI Quanta 200). A cross section of the film and the substrate was obtained with Focused Ion Beam equipment (Zeiss 1560XB Cross Beam) at 30 kV and 50 pA using Ga ions.

The interfacial adhesion of C and C/SiO_2 films to Si substrates was assessed by observing the eventual detachment of the films from the substrate after submitting them to an ultrasonic treatment in an acetone bath for 3 min. The interfacial adhesion was also characterized by an additional peeling test. Before performing the test, the substrates were glued on a microscope glass slide using silver paste. A piece of a transparent tape (MagicTM from 3M) was scotched onto the film and then peeled off while holding the glass slide.

Four-point probe measurements were carried out to determine the sheet resistance of the C/SiO_2 films. Three measurements were performed on different areas of each sample and the film thickness determined on an area of 200 μm × 200 μm by profilometry. From the profilometric measurement, the maximum, the minimum and the average value were considered to calculate the conductivity values from the sheet resistance. The conductivity value was determined as the average of those nine values and its standard deviation was considered its error. The electrochemical performance of the C/SiO_2 films was investigated by assessing the cyclic voltammetric behavior of the ferricyanide/ferrocyanide redox couple in 0.1 M KNO_3 solutions using a Autolab unit controlled GPES software (Metrohm-Autolab B.V., The Netherlands). In order to carry out these measurements, the film area to be used as the working electrode was defined by gluing a 3 mm diameter cylindrical plastic cuvette to the film surface using thermoplastic silicone. Electrical contact was done by fixing an Al wire on one corner of the film with silver paste (see Figure S3 for a schematic drawing of the setup). When carrying out the measurements, a silver wire pseudoreference electrode and a stainless steel wire counter electrode were immersed in the cuvette to complete the electrochemical cell.

3. RESULTS AND DISCUSSION

3.1. Sol−Gel Synthesis of C/SiO_2 Films on Si Substrates. As can be seen in Table 1, the incorporation of APTES into resorcinol/formaldehyde system accelerates gelation. Keeping constant the acetic acid content, the gelation time decreased significantly by increasing the relative content of APTES from 0.2 to 0.5. For instance, CS11-$A_{H\text{-}1}$ gelled after only ∼0.15 h, but crack-free films could not be obtained with this sol. To facilitate sol handling and processing into a film by spin coating, gelation rate was thus slowed down by doubling the volume of solvent. Acids are catalysts for both resorcinol/formaldehyde and silica sol−gel processes. However, the gelation rate of resorcinol/formaldehyde/APTES system was observed to increase dramatically by decreasing the acetic acid content. For instance, in the case of the C/SiO_2 CS41 film series, the gelation time decreased from 72 h to 30 min with the absence of 785 μL acetic acid. This paradoxical behavior can be understood if one takes into account that gels are also base-catalyzed and that the presence of an amino group in APTES chemical structure provides base characteristics to the compound. The amino group catalyzes inter- or intramolecular reactions between silane molecules and silanol groups to form siloxane bonds, one of the necessary steps of the resorcinol/formaldehyde/APTES gelation process. The slowing down in the gelation rate induced by the addition of acetic acid occurs because it neutralizes the basic character of the amino group weakening its catalytic effect.

The carbonization processes involved a large reduction of the vertical film dimensions. Taking sample CS21-A_H as an example, the average thickness of the film decreased from ∼900 to ∼400 nm, that is, ∼55% reduction in thickness. Taking into account the fact that the SiO_2 xerogel shrinks less than the resorcinol/formaldehyde xerogel during pyrolysis, it was expected that shrinkage decreases for samples containing more SiO_2. Indeed, in the case of sample CS11-A_H, which contains the largest amount of SiO_2, a ∼50% reduction in thickness was observed. Even though the presence of acetic acid in the CS41 sample series significantly slowed down the gelation rate, we did not observe any influence of this parameter on the film shrinkage. Interestingly, thanks to the strong interfacial adhesion between C/SiO_2 film and the silicon/silicon oxide substrate, none of the studied C/SiO_2 films showed shrinkage in the lateral dimensions regardless the dimensions of the used substrates. In spite of the important shrinkage resulting from pyrolysis, the C/SiO_2 films are expected to present a substantial porosity. Even though this could not be characterized by standard methods due to the small mass of the films, we investigated the porosity of bulk C/SiO_2 materials by nitrogen adsorption porosimetry. In the case of the bulk CS41 monoliths the porosity is characterized by the presence of pores below 3 nm (micropores) and a surface area of 120 m^2/g (see Figure S4).

3.2. Interfacial Adhesion between the Films and the Si Substrate. Taking into consideration the eventual film application as electrochemical sensors working in liquid solutions, we first carried out a liquid test under tough conditions to assess the film adhesion to the substrate. Two films (with and without SiO_2) were immersed in acetone and placed in an ultrasonic bath for 3 min. Figure 1 shows the images of the films after the test. It can be clearly observed that the pure carbon film (C-A), peels off from the Si substrate, demonstrating a very poor interfacial adhesion. By contrast, the C/SiO_2 film (C41-A_L) shows no flaws after the ultrasonic treatment, indicating that the addition of SiO_2 significantly enhances the film interfacial adhesion. We hypothesize that this fact is directly related to the formation of Si−O−Si covalent bonds between the SiO_2 xerogel and the SiO_2 layer on the silicon substrate. Moreover, it can also be said from Figure 1 that a R/APTES molar ratio of 1/4 creates a C/SiO_2 thin films

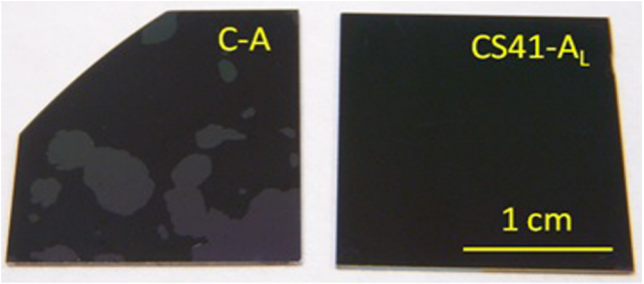

Figure 1. Representative images of pure carbon and C/SiO_2 films on Si substrates after ultrasonic treatment in acetone bath for 3 min.

DOI: 10.1021/acsami.6b07347
ACS Appl. Mater. Interfaces 2016, 8, 31092−31099

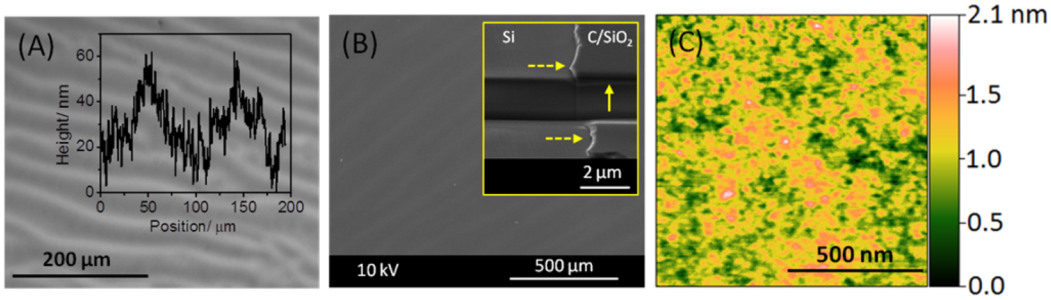

Figure 2. Representative optical (A), SEM (B), and AFM (C) images of the C/SiO_2 thin films. The inset of panel A is the extracted surface profile scanned by profilometer. The inset of panel B is the SEM image of a cross-section of the film created by intentionally scratching the film from top to bottom (see dotted yellow arrows) and a cross-section of the film and the substrate along the left−right direction performed using FIB (solid yellow arrow).

with an interfacial adhesion strong enough to withstand immersion processes in aqueous solutions and still carry out electrochemical measurements. Indeed, except for C-A film, no film detachment was observed in any of the hybrid C/SiO_2 film samples listed in Table 1.

More evidence on the enhanced adhesion of the C/SiO_2 films compared to C films was obtained with peeling tests using scotch tape (see Movies S1 and S2). The movies unambiguously show that the C film is peeled off from the substrate with the tape while this is not the case for the C/SiO_2 film.

3.3. Topography of the Carbon Thin Films. Figure 2A shows a representative optical image of a C/SiO_2 thin film and the corresponding surface profile recorded with a profilometer. It shows that the film surface is not flat as it presents roughness at two scales: a wave-like roughness morphology with an amplitude of about 50 nm and a periodicity of about 50 μm onto which a surface roughness of smaller vertical and lateral dimensions can be detected. This is a common feature of spin coated films and is likely to be related to the rapid drying of the deposited film during the spin-coating process, especially when a volatile solvent with low boiling point such as ethanol is used.[23] In addition, we found that the wave-like roughness becomes more pronounced for thicker films. For instance, the wave amplitude increased from 40 to 70 nm as the thickness of the CS21-A_H C/SiO_2 film increased from 400 to 800 nm. It was also found that in films of different composition but comparable thicknesses, the SiO_2 content had little effect on the wave amplitude. At this point, it should be emphasized that the motivation of our work was developing C/SiO_2 films to be further patterned by photolithographic techniques into miniaturized electrodes for electrochemical sensing. The ∼50 nm wavelike roughness is expected to have a negligible influence on the patterning process considering the overall C/SiO_2 film thickness (between 400 and 800 nm) and the usual thickness of the photoresists required to produce patterns in the micron range (between 1 and 5 μm).

Figure 2B shows a characteristic SEM image of a film in planar view that displays the above-mentioned wave-like roughness and no cracks. The inset of Figure 2B shows cross sections of the film in the vertical direction, and of the film and the Si substrate along the horizontal direction. The creation of these cross-sectional features did not result in any crack formation at the film−substrate interface or on the surface of the film, this providing further evidence of the film robustness.

Atomic force microscopy (AFM) was used to analyze the surface roughness of the C/SiO_2 films with an increased lateral resolution. Figure 2C shows a typical AFM image recorded on the CS41 sample, for which a surface roughness value of around 0.2 nm was obtained. The surface roughness measured by AFM became larger in the films with higher SiO_2 content. For instance, the roughness value increases up to ∼1 nm for the sample CS11-A_H with the largest SiO_2 content. Nevertheless, for the targeted application, the roughness of these C/SiO_2 films can be considered small and its homogeneity excellent as any phase separation between carbon and SiO_2 components was not observed at the macro and microscales by scanning electron microscopy analysis using the backscattered electrons mode, which reveals an intensity contrast when changes in the average atomic number exist in the studied materials. Further insight into the microstructure of the C/SiO_2 films could be obtained by selectively etching the SiO_2 in a 2 M NaOH aqueous solution. After immersing the films for 2 h in this solution, the SEM images reveal a highly branched dendritic-like structure with voids between the branches, formerly occupied by the SiO_2, with lateral dimensions below the micron range (see Figure S5). Extending the immersion time results in the complete detachment of the film and makes the solution to acquire a dark tone as a result of the carbon debris present in suspension. These observations indicate that the film structure includes two independent intermixed networks of C and SiO_2, resulting from the polymerization of resorcinol and formaldehyde and the hydrolysis and condensation of APTES, respectively. Such interwoven C and SiO_2 networks are responsible for the increased robustness of the films thanks to the strong attachment of SiO_2 to the substrate through silanol bonds. Regarding the nature of the intermixed networks, we considered the possibility of the amine moiety present in APTES participating in the enhanced robustness of the films by creating a chemically bonded C/SiO_2 interface, as it has been reported that alkyl amines can be bonded to glassy carbon.[24,25] We could not find evidence of N−C−Si bonding from XPS measurements (see Figure S6). These measurements revealed that N was not present in the C-SiO_2 films, even though it was detected in the gel films before pyrolysis, indicating a thermal decomposition of the amine moieties.

3.4. Electrical Conductivity of the C/SiO_2 Thin Films. The addition of APTES made the deposition of C/SiO_2 thin films much easier and more efficient in terms of reaction time than that of pure carbon films and also strongly improved their interfacial adhesion to silicon/silicon oxide substrate. However, the presence of SiO_2 hinders the charge transport through carbon, resulting in a higher electrical resistivity of C/SiO_2 compared to that of the pure carbon film. Figure 3 presents the

DOI: 10.1021/acsami.6b07347
ACS Appl. Mater. Interfaces 2016, 8, 31092−31099

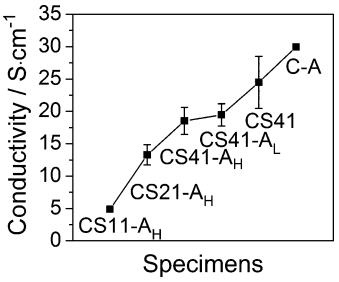

Figure 3. Electrical conductivities of C/SiO_2 films containing different of SiO_2 content or prepared from sols with different concentrations of acetic acid.

electrical conductivity of the different C/SiO_2 thin films. The electrical conductivities reported in the literature for carbon xerogel and aerogel materials pyrolyzed at 1000 °C vary from 1 to 40 S·cm^{-1}.[26] Here, the electrical conductivity for the pure carbon xerogel film is ~30 S·cm^{-1}. The electrical conductivity decreases with the increase of the SiO_2 content. For instance, the conductivities measured for the films CS41-A_H and CS11-A_H, which contain the lowest and highest amount of SiO_2 in the CS-A_H series, are around 5 and 18 S·cm^{-1}, respectively. Nevertheless, the conductivity of these C/SiO_2 films are quite comparable to or even higher than that of typical screen printed carbon inks used in electrochemical sensing whose reported values are between 1 and 10 S·cm^{-1}.[27] One can expect that the conductivity measurements were affected by the existence of the 50 nm wavelike roughness described above. An estimation of the relative error related to such variations for a typical thickness of 400 nm results in a relative error of about 12%, in agreement with the larger errors experimentally determined, except for CS41 films.

Figure 3 also shows that the film prepared from a sol without acetic acid (CS41) shows a somewhat higher electrical conductivity than those with the same C/SiO_2 composition but prepared from sols containing acetic acid (CS41-A_H and CS41-A_L). This conductivity change is due to differences in the surface chemical composition of the films, which were revealed by a comparative XPS analysis of the CS41 and CS41-A_H films. Figure 4 presents the normalized XPS spectra corresponding to the C 1s, O 1s, and Si 2p of these two films. The CS41-A_H film shows higher relative intensities of the Si 2p and O 1s peaks and correspondingly a lower relative intensity of the C 1s peak. In Figure 4c one can also note that the shapes of the Si 2p spectra of the two films are quite different. Using Gaussian curve fitting, the Si 2p spectrum of both films can be decomposed into two peaks ascribed to oxidized silicon and centered at around 103.4 and 101.9 eV (see inset of Figure 4c). The 103.4 eV peak corresponds to SiO_2 whereas the 101.9 eV peak falls in the binding energy range of the suboxides (SiO_x, with $x < 2$). Interestingly, the relative SiO_x content is much higher in CS41 film than in CS41-A_H film. This supports our hypothesis that the presence of acetic acid alters the gelation process of APTES by blocking the catalytic effect of amino group and thus making the gelation slower.

To get a better insight into this mechanism and avoiding the complexity of gelation studies in films we investigated the formation of bulk monolithic gels from the CS41 and CS41-A_H sols. The monitoring of the resorcinol/formaldehyde/APTES sols without and with acetic acid at different stages of the gelation process gave valuable information to understand the differences observed in the films (see images of different stages

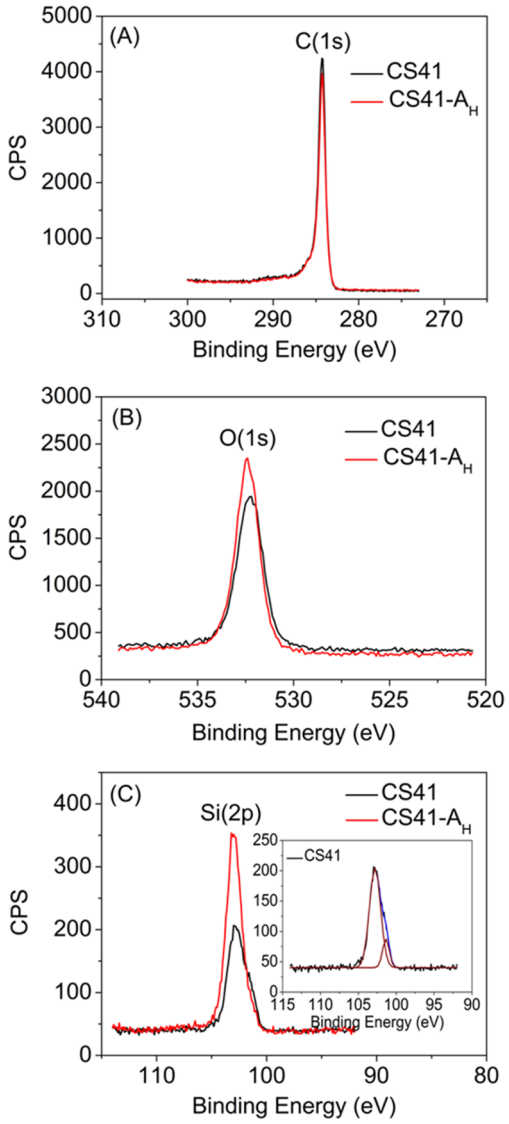

Figure 4. XPS spectra of showing the binding energies of C 1s (A), O 1s (B), and Si 2p (C) for the CS41 and CS41-A_H films.

of the process in Figure S3). On one hand, at a given reaction time the color of the CS41 sol was darker than that of CS41-A_H sol, confirming the faster gelation of CS41 system. On the other hand, during the aging stage following the gelation process, we observed that the gel of CS41-A_H showed a homogeneous appearance whereas the color of the CS41 gel was lighter at the bottom and darker at the top. As we know, SiO_2 gels are normally white and resorcinol/formaldehyde gels are red in color. The homogeneous color of the CS41-A_H system during the whole process reveals a simultaneous formation of resorcinol/formaldehyde and APTES networks. By contrast, for the CS41 system the gel was first white and then gradually turned to red but showing a color gradient from the top to the bottom of the gel, evidencing the initial gelation of APTES later followed by the formation of resorcinol/formaldehyde gel. Thus, in the CS41 system, the initially formed SiO_2 network tends to form clusters[28] because it is base-catalyzed, and those are dragged toward the bottom of the container because of its higher density and the resulting gel is not homogeneous. If this phenomenon is extrapolated to the formation of gel films by spin coating, one can understand the higher relative SiO_2

DOI: 10.1021/acsami.6b07347
ACS Appl. Mater. Interfaces 2016, 8, 31092−31099

content at the surface of the CS41-A_H film and its lower conductivity.

3.5. Electrochemical Performance of the C/SiO_2 Thin Films. Figure 5 displays typical voltammograms recorded with

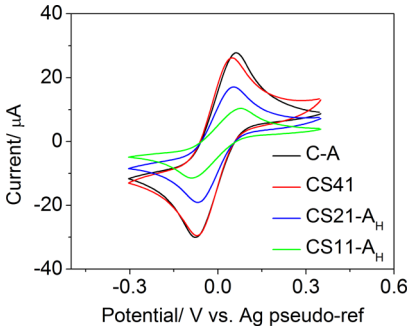

Figure 5. Cyclic voltammograms recorded with C/SiO_2 films with different silica content, in a 0.1 M KNO_3 solution containing 1 mM ferri/ferrocyanide redox couple. Scan rate: 50 mV/s.

the C/SiO_2 films. Quasi-reversible electrochemical responses were recorded, showing an anodic to cathodic peak current ratio of around 1. It was also observed that the peak to peak potential separation (ΔE_P) appreciably decreases from ~167 to 137 mV when the molar fraction of APTES in the films decreased from 0.5 to 0.2 while, by contrast, the faradic peak currents increased from 10/−11 to 26/−29 μA, respectively. The higher peak current and lower ΔE_P indicate a larger active surface area and a faster electron transfer at the electrolyte C/SiO_2 film interface. This is the expected behavior taking into account the higher conductivity of the films with lower silica content. Surprisingly, pure carbon films (C−A) showed a similar peak current but larger ΔE_P compared to those recorded with CS41 films. This might be related to the differences in the surface chemistry and hence to the interaction of the ferri/ferrocyanide redox probes with the film surface, which is well-known to greatly influence the electron transfer and so the resulting electrochemical performance.[29,30] As thoroughly reported by McCreery et al.,[30] carbon electrode materials get easily oxidized in air and the oxygen-containing functionalities are mostly responsible for the different electrode surface chemistry and thus for the electrochemical performance assessed with these redox species. In this context, the solution pH also plays an important role on the voltammetric behavior of ferri/ferrocyanide. This effect was also shown in the study carried out with the CS41 film (see Figure S8). Electrical repulsion with negatively charged oxygen species at alkaline pHs and the formation of Prussian Blue complex at acidic pHs, indicated by the generation of a blue color in the measuring solution, may be responsible for the differences in the recorded cyclic voltammetric responses. In addition, this study demonstrates the successful electrochemical behavior of the films when working at different solution pHs, this being relevant for electroanalytical purposes.

The influence of the scan rate on the voltammetric responses recorded with the CS41 film was also studied with the CS41 film. The corresponding peak currents (see Figure S9) are proportional to the square-root of the scan rate in the range of 10−100 mV/s, which is the usual behavior of a diffusion-controlled electrode process.

Figure 6 compares the cyclic voltammetric response of the CS41 film electrode prepared in this work, with those of a

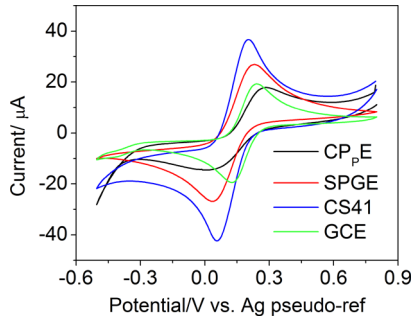

Figure 6. Cyclic voltammograms recorded in a 0.1 M KNO_3 solution containing 1 mM ferri/ferrocyanide redox couple at C_PPE, SPGE, GC, and CS41 at a scan rate of 50 mV/s.

porous carbon xerogel paste electrode (C_PPE) as prepared in our previous publication,[19] a commercial screen printed graphite electrode (DRP 110 from DropSens S.L, Spain; SPGE), and a commercial glassy carbon electrode (CH Instruments Inc., US; GCE). At a scan rate of 50 mV/s, ΔE_P values of around 137, 210, 181, 107 mV were measured, respectively. Compared to C_PPE and SPGE, a much smaller ΔE_P value was recorded with CS41 film electrode, indicating a relatively faster electron transfer at the film electrolyte interface. The heterogeneous electrochemical rate constant k^0 was also calculated for the four tested devices using the Nicholson method (eq 1).[31]

$$\varphi = k^0[\pi DnvF/(RT)]^{-1/2} \quad (1)$$

where D is the diffusion coefficient of potassium ferricyanide in 0.1 M KNO_3 (~7.01×10^{-6} $cm^2 \cdot s^{-1}$),[32] n is the number of electrons involved in the electrochemical reaction, which in this case is equal to one, ν is the scan rate in V/s, F is the faraday constant, R is the universal gas constant, and T the absolute temperature. The dimensionless kinetic parameter, φ, is first determined using the following analytical equation:

$$\varphi = (-0.6288 + 0.0021\Delta E_p)/(1 - 0.017\Delta E_p) \quad (2)$$

The electrochemical performance of the different types of electrodes, described by the ΔE_P and k^0 values, is reported in Table 2. The k^0 for CS41 film was 0.0017 cm/s. This value

Table 2. Peak Separation and Electron Transfer Rate k^0 value for different electrodes in a 0.1 M KNO_3 solution containing 1 mM ferri/ferrocyanide redox couple

electrode type	ΔE_P (mV)	k_0 (cm/s)
CS41 C/SiO_2	137	0.0017
CS21-A_H C/SiO_2	155	0.0012
CS11-A_H C/SiO_2	167	0.0010
SPGE	181	0.0008
C_PPE	210	0.0005
GCE	107	0.0032

accounts for a quite favorable electron transfer rate compared to that of SPGE and C_PPE, whose estimated k^0 values were 0.0008 and 0.0005 cm/s, respectively. In addition, the k^{00} values for CS21-A_H and CS11-A_H films were estimated to be 0.0012 and 0.0010 cm/s, respectively. Thus, larger SiO_2 contents of the films give rise to slower transfer kinetics. Nevertheless, these are still significantly higher than those calculated for SPGE and C_PPE. Additionally, it has been reported that the electron

DOI: 10.1021/acsami.6b07347
ACS Appl. Mater. Interfaces 2016, 8, 31092−31099

transfer rate k^0 value typically ranges from 10^{-4} to 10^{-2} cm/s at carbon based electrodes,[33] depending on the structure and morphology of carbon materials. The CS41 film electrode underperforms the electrochemical behavior of the commercial GCE, which shows smaller ΔE_P and a larger k^0 value of 0.0032 cm/s. It is worth mentioning that, the developed CS41 film electrodes as well as the GCE do not contain any extra additives such as paraffin and curing binders, that by contrast are incorporated in the C_PPE and SPGE compositions, respectively, and which are shown to be detrimental to the electrochemical performance of the resulting electrode devices.

4. CONCLUSION

This study describes the production of robust thin carbon films on silicon substrates by a one-pot resorcinol/formaldehyde/APTES sol−gel spin coating approach. The inclusion of acid in the sol influences the deposition and the final properties of the films. The interfacial adhesion between carbon films and silicon substrates can be significantly enhanced by the addition of a SiO_2 precursor to the sol formulation. The carbon/silica films display a uniform appearance. By contrast, they present a phase segregation between carbon and silica in the form of interwoven dendritic-like networks below the micron range. Compared to pure carbon xerogel films, the addition of SiO_2 was not detrimental to the functional properties of the films, showing conductivities larger than those reported for typical screen printed inks. Cyclic voltammetry studies demonstrate the great potential of this material in electroanalytical chemistry, with the additional advantage of its prospective application in the fabrication of carbon/silica thin-film electrodes by photolithographic processes. For such application, CS41 appears as the most suitable among all the materials studied herein, as it shows the highest conductivity and a short reaction time that allows obtaining films only 10 min after preparing the sol. Moreover, the CS41 films show superior performance close to that of commercial glassy carbon electrodes.

■ ASSOCIATED CONTENT

Supporting Information

The Supporting Information is available free of charge on the ACS Publications website at DOI: 10.1021/acsami.6b07347.

Cracks in C/SiO_2 films; profilometry of C/SiO_2 film; electrochemical testing setup; porosity of bulk C/SiO_2 monolith; microstructure of C/SiO_2 films; XPS spectra of C/SiO_2 films before and after pyrolysis; influence of acetic acid in the gelation of resorcinol−formaldehyde/APTES sols; cyclic voltammetries at different solution pH; cyclic volatmmetries at different scan rates (PDF)

Peeling test of the adhesion of the C films (AVI)

Peeling test adhesion of the C/SiO_2 films (AVI)

■ AUTHOR INFORMATION

Corresponding Authors

*E-mail: mgich@icmab.es

*E-mail: cesar.fernandez@imb-cnm.csic.es

Notes

The authors declare no competing financial interest.

■ ACKNOWLEDGMENTS

Guillermo Antorrena from the Laboratorio de Microscopias Avanzadas of the Instituto de Nanociencia de Aragón and Guillaume Sauthier from Institut Català de Nanociència i Nanotecnologia are acknowledged for performing XPS analysis. We thank Ander Arbide for performing peeling tests. This research was partially funded by, the European Union's 7th Framework Programme (FP7/2007-2013) under grant agreement number 614155, the Spanish Ministry of Economy and Competitiveness in cofounding with the European Social Funds through the MAT2015-64442-R project, the "Severo Ochoa" Programme for Centres of Excellence in R&D (SEV-2015-0496) and the Generalitat de Catalunya (2014SGR213, 2014SGR1645). The Chinese Scholarship Council fellowship (201206240033) to P.N. and the COST Action MP1202 are also acknowledged.

■ REFERENCES

(1) McCreery, R. L. Advanced Carbon Electrode Materials for Molecular Electrochemistry. *Chem. Rev.* **2008**, *108*, 2646−2687.

(2) Zhang, W.; Zhu, S. Y.; Luque, R.; Han, S.; Hu, L. Z.; Xu, G. B. Recent Development of Carbon Electrode Materials and Their Bioanalytical and Environmental Applications. *Chem. Soc. Rev.* **2016**, *45*, 715−752.

(3) Kinoshita, K. *Carbon: Electrochemical and Physicochemical Properties*; Wiley: New York, 1988.

(4) Baptista, F. R.; Belhout, S. A.; Giordani, S.; Quinn, S. J. Recent Developments in Carbon Nanomaterial Sensors. *Chem. Soc. Rev.* **2015**, *44*, 4433−4453.

(5) Mao, X.; Rutledge, G. C.; Hatton, T. A. Nanocarbon-Based Electrochemical Systems for Sensing, Electrocatalysis, and Energy Storage. *Nano Today* **2014**, *9*, 405−432.

(6) Banks, C. E.; Compton, R. G. New Electrodes for Old: from Carbon Nanotubes to Edge Plane Pyrolytic Graphite. *Analyst* **2006**, *131*, 15−21.

(7) Brownson, D. A. C.; Kampouris, D. K.; Banks, C. E. Graphene Electrochemistry: Fundamental Concepts Through to Prominent Applications. *Chem. Soc. Rev.* **2012**, *41*, 6944−6976.

(8) Švancara, I.; Vytřas, K.; Kalcher, K.; Walcarius, A.; Wang, J. Carbon Paste Electrodes in Facts, Numbers, and Notes: A Review on the Occasion of the 50-Years Jubilee of Carbon Paste in Electrochemistry and Electroanalysis. *Electroanalysis* **2009**, *21*, 7−28.

(9) Newman, J. D.; Turner, A. P. F. Home Blood Glucose Biosensors: a Commercial Perspective. *Biosens. Bioelectron.* **2005**, *20*, 2435−2453.

(10) Dominguez Renedo, O.; Alonso-Lomillo, M. A.; Arcos Martinez, M. J. Recent Developments in the Field of Screen-Printed Electrodes and Their Related Applications. *Talanta* **2007**, *73*, 202−219.

(11) Wang, J. Decentralized Electrochemical Monitoring of Trace Metals: From Disposable Strips to Remote Electrodes: Plenary Lecture. *Analyst* **1994**, *119*, 763−766.

(12) Niwa, O. Electroanalytical Chemistry with Carbon Film Electrodes and Micro and Nano-structured Carbon Film-based Electrodes. *Bull. Chem. Soc. Jpn.* **2005**, *78*, 555−571.

(13) Wang, C.; Zhang, J.; Ryu, K.; Badmaev, A.; De Arco, L. G.; Zhou, C. Wafer-Scale Fabrication of Separated Carbon Nanotube Thin-Film Transistors for Display Applications. *Nano Lett.* **2009**, *9*, 4285−4291.

(14) Zhang, L.; Shi, Z.; Wang, Y.; Yang, R.; Shi, D.; Zhang, G. Catalyst-Free Growth of Nanographene Films on Various Substrates. *Nano Res.* **2011**, *4*, 315−321.

(15) McFadden, C. F.; Russell, L. L.; Melaragno, P. R.; Davis, J. A. Low-Temperature Pyrolytic Carbon Films: Electrochemical Performance and Surface Morphology as a Function of Pyrolysis Time, Temperature, and Substrate. *Anal. Chem.* **1992**, *64*, 1521−1527.

(16) Jung, C. H.; Kim, W. J.; Jung, C. H.; Hwang, I. T.; Khim, D.; Kim, D. Y.; Lee, J. S.; Ku, B. C.; Choi, J. H. A Simple PAN-Based Fabrication Method for Microstructured Carbon Electrodes for Organic Field-Effect Transistors. *Carbon* **2015**, *87*, 257−268.

DOI: 10.1021/acsami.6b07347
ACS Appl. Mater. Interfaces 2016, 8, 31092−31099

(17) Kim, J.; Song, X.; Kinoshita, K.; Madou, M.; White, B. Electrochemical Studies of Carbon Films from Pyrolyzed Photoresist. *J. Electrochem. Soc.* **1998**, *145*, 2314−2319.
(18) Bohannan, E. W.; Gao, X. R.; Gaston, K. R.; Doss, C. D.; Sotiriou-Leventis, C.; Leventis, N. Photolithographic Patterning and Doping of Silica Xerogel Films. *J. Sol-Gel Sci. Technol.* **2002**, *23*, 235−245.
(19) Gich, M.; Fernandez-Sanchez, C.; Cotet, L. C.; Niu, P.; Roig, A. Facile Synthesis of Porous Bismuth-Carbon Nanocomposites for the Sensitive Detection of Heavy Metals. *J. Mater. Chem. A* **2013**, *1*, 11410−11418.
(20) Ye, L.; Ji, Z. H.; Han, W. J.; Hu, J. D.; Zhao, T. Synthesis and Characterization of Silica/Carbon Composite Aerogels. *J. Am. Ceram. Soc.* **2010**, *93*, 1156−1163.
(21) Song, L.; Feng, D.; Campbell, C. G.; Gu, D.; Forster, A. M.; Yager, K. G.; Fredin, N.; Lee, H. J.; Jones, R. L.; Zhao, D.; Vogt, B. D. Robust Conductive Mesoporous Carbon-Silica Composite Films with Highly Ordered and Oriented Orthorhombic Structures from Triblock-Copolymer Template Co-assembly. *J. Mater. Chem.* **2010**, *20*, 1691−1701.
(22) Si, M.; Feng, D.; Qiu, L.; Jia, D.; Elzatahry, A. A.; Zheng, G.; Zhao, D. Free-standing Highly Ordered Mesoporous Carbon-Silica Composite Thin Films. *J. Mater. Chem. A* **2013**, *1*, 13490−13495.
(23) Spangler, L. L.; Torkelson, J. M.; Royal, J. S. Influence of Solvent and Molecular-Weight on Thickness and Surface-Topography of Spin-Coated Polymer-Films. *Polym. Eng. Sci.* **1990**, *30*, 644−653.
(24) Deinhammer, R. S.; Ho, M.; Anderegg, J. W.; Porter, M. D. Electrochemical Oxidation of Amine-Containing Compounds: a Route to the Surface Modification of Glassy Carbon Electrodes. *Langmuir* **1994**, *10*, 1306−1313.
(25) Nasir, T.; Zhang, L.; Vilà, N.; Herzog, G.; Walcarius, A. Electrografting of 3-Aminopropyltriethoxysilane on a Glassy Carbon Electrode for the Improved Adhesion of Vertically Oriented Mesoporous Silica Thin Films. *Langmuir* **2016**, *32*, 4323−4332.
(26) Fung, A. W. P.; Wang, Z. H.; Lu, K.; Dresselhaus, M. S.; Pekala, R. W. Characterization of Carbon Aerogels by Transport Mesaurements. *J. Mater. Res.* **1993**, *8*, 1875−1885.
(27) See for instance Product Specifications of Commercial Carbon Inks at Gwent Group, Carbon Working Electrode Materials. http://www.gwent.org/gem_carbon_working.html (accessed Jul 5 2016).
(28) Wright, J. D.; Sommerdijk, N. A. J. M. *Sol−Gel Materials: Chemistry and Applications*. CRC Press: London, 2000.
(29) McCreery, R. L.; McDermott, M. T. Comment on Electrochemical Kinetics at Ordered Graphite Electrodes. *Anal. Chem.* **2012**, *84*, 2602−2605.
(30) Chen, P.; McCreery, R. L. Control of Electron Transfer Kinetics at Glassy Carbon Electrodes by Specific Surface Modification. *Anal. Chem.* **1996**, *68*, 3958−3965.
(31) Nicholson, R. S. Theory and Application of Cyclic Voltametry for Measurement of Electrode Reaction Kinetics. *Anal. Chem.* **1965**, *37*, 1351−1355.
(32) Griffiths, K.; Dale, C.; Hedley, J.; Kowal, M. D.; Kaner, R. B.; Keegan, N. Laser-Scribed Graphene Presents an Opportunity to Print a New Generation of Disposable Electrochemical Sensors. *Nanoscale* **2014**, *6*, 13613−13622.
(33) Lee, S. H.; Fang, H. Y.; Chen, W. C.; Lin, H. M.; Chang, C. A. Electrochemical Study on Screen-Printed Carbon Electrodes with Modification by Iron Nanoparticles in Fe(CN)(6)(4-/3-) Redox System. *Anal. Bioanal. Chem.* **2005**, *383*, 532−538.

DOI: 10.1021/acsami.6b07347
ACS Appl. Mater. Interfaces 2016, 8, 31092−31099